International Journal of Heat and Mass Transfer 52 (2009) 281–288

Contents lists available at ScienceDirect

International Journal of Heat and Mass Transfer

journal homepage: www.elsevier.com/locate/ijhmt

Convective heat transfer and pressure losses across novel heat sinks fabricated by Selective Laser Melting

M. Wong [a,*], I. Owen [a], C.J. Sutcliffe [a], A. Puri [b]

[a] Department of Engineering, University of Liverpool, Liverpool L69 3GH, UK
[b] Selex Sensors and Airborne Systems Ltd, 300 Capability Green, Luton LU1 3PG, UK

ARTICLE INFO

Article history:
Received 24 October 2007
Received in revised form 11 March 2008
Available online 21 July 2008

Keywords:
Heat sink
Pin fin
Offset strip
Lattice
Rapid prototyping
Selective Laser Melting

ABSTRACT

This study presents the thermal and fluid flow characteristics of five heat sinks that have been fabricated by a rapid manufacturing technique known as Selective Laser Melting. The five heat sinks consist of two conventional designs, the cylindrical pin and rectangular fin array, for comparison purposes, and three novel heat sinks: a staggered elliptical array; a lattice; and a rectangular fin array with rounded corners. The experimental results for the rectangular fin were compared with data from the literature and were found to be consistent. The rectangular fin with rounded corners proved able to transfer the largest amount of heat whilst improving upon the pressure drop performance of the standard rectangular fin array. Although the lattice arrangement made use of the fabrication process' ability to manufacture heat sinks with high surface area to volume ratios, its performance was limited by the lack of interaction between the cooling air and structure. In terms of both heat transfer performance and pressure drop, the staggered elliptical array, which cannot be manufactured by conventional techniques, outperformed the other heat sinks.

1. Introduction

Forced convection cooling is a process commonly found in a variety of consumer and industrial electronic products ranging from personal computers to avionics control systems. Heat is removed from a component and dissipated into a fluid that can be blown or pumped away to maintain favourable working temperatures, and therefore reliable electronic systems. As electronic components continue to dissipate more heat with new developments, cooling techniques must also improve for these components to stay within the required temperature limits.

A common method of cooling is to use extended surfaces (fins) with air or liquid as the heat-carrying medium. For simplicity, reliability and cost, air is often the favoured option; all that is required to cool a component is a fan and a heat sink. Heat sinks are passive devices that absorb heat and dissipate it to a cooling fluid using extended surfaces. The surfaces come in a variety of geometries; some of the more common ones being cylindrical pin fins, strip fins and plate fins.

The main concerns when selecting a heat sink are its heat transfer performance and the resistance to air flow across its extended surfaces. Secondary to these criteria are application-specific requirements such as cost, mechanical strength and mounting techniques. For example, extended surfaces employed in turbine blades or avionics cold walls must be able to withstand mechanical stresses using geometries that can be cast as part of the overall blade or chassis. Cylindrical pin fins are the favoured option for these applications; their performance is also less dependent on the coolant flow direction when compared to other geometries. Research on cylindrical extended surfaces often uses empirical data for long tubes gathered by Zukauskas [1] as a starting point but the work of Brigham and Van Fossen [2], Metzger et al. [3], Peng [4], and Armstrong and Winstanley [5] concentrates on pressure and heat transfer correlations specifically for short pin arrays heated from both sides. The work of Babus'Haq et al. [6], Short [7], Sparrow et al. [8] and Tahat et al. [9,10] concentrates on pin fins heated from one side only to represent the situation in an electronics cooling environment.

The strip fin is another extended surface design that has been extensively investigated by De Jong et al. [11], Joshi and Webb [12], and Zhang et al. [13] through both experimental and computational methods. Two mechanisms act to improve heat transfer from an offset strip fin compared with that of a plate fin. First, the interruptions prevent the thickening of the boundary layer and, second, the interruptions cause oscillations in the flow, thereby enhancing heat transfer by generating vortices that force cooler fluid toward the fin [11].

The heat transfer and pressure drop characteristics of both the strip fin and pin fin are well established, principally because their

* Corresponding author.
E-mail address: m.wong@liverpool.ac.uk (M. Wong).

0017-9310/$ - see front matter © 2008 Elsevier Ltd. All rights reserved.
doi:10.1016/j.ijheatmasstransfer.2008.06.002

Nomenclature

a	pin length in flow direction (mm)
A	heat transfer surface area (mm^2)
A_{prime}	prime surface area (mm^2)
A_{ff}	flow area at minimum cross section (mm^2)
b	pin width (mm)
c_p	specific heat capacity of air (J kg^{-1} K^{-1})
d	pin diameter (mm)
D_h	hydraulic diameter (mm)
f	friction factor (dimensionless)
h	heat transfer coefficient (W/m^{-2} K^{-1})
h_{mod}	modified heat transfer coefficient (W/m^{-2} K^{-1})
j	j-factor (dimensionless)
H	pin height/length (mm)
k	thermal conductivity of air (W/m^{-1} K^{-1})
L	heat sink length in flow direction (mm)
$\dot{m}$	air mass flow rate (kg s^{-1})
Nu	Nusselt number (dimensionless)
Re	Reynolds number (dimensionless)
S	pin streamwise spacing (mm)
T	pin transverse spacing (mm)
T_{base}	heat sink base temperature (°C)
T_{in}	inlet temperature (°C)
T_{out}	outlet temperature (°C)
T_s	heat sink surface temperature (°C)
T_∞	bulk mean air temperature through heat sink (°C)
V_{ff}	air velocity at minimum cross section (m s^{-1})

Greek Symbols

Δp	pressure drop (Pa)
μ	dynamic viscosity of air (kg m^{-1} s^{-1})
ρ	density of air (kg m^{-3})

geometries can be easily manufactured using traditional fabrication techniques such as milling, die-casting, forging, folding or brazing, or a combination of processes [14]. Other studies have investigated extended surfaces which are more challenging to manufacture.

The elliptical fin array was considered by Matos et al. [15] and shown to provide a 13% increase in heat transfer and a 25% reduction in pressure loss when compared with an optimal cylinder array. Chen et al. [16] showed that drop-shaped pins offer heat transfer rates up to 29% higher than their cylindrical counterparts, with only half the pressure drop. The heat transfer characteristics of cellular metals have also been investigated, for example by Bastawros et al. [17], Lu [18] and Zhao et al. [19]. The high thermal conductivity of the metal combined with the eddies generated within the foam act to provide about five times the heat transfer when compared to a pin fin array, but with the added penalty of high pressure drop. Lattice type materials consisting of angled cylinders were investigated by Kim et al. [20–22] for applications where heat sinks are also required to carry structural loads; their performance was found to be similar to that of a bank of cylinders.

Previous research into less conventional extended surfaces shows that there are performance gains to be achieved by considering more novel heat sink shapes, but progress is limited due to manufacturing constraints. This paper introduces a rapid manufacturing process, Selective Laser Melting, which provides the heat transfer researcher with a technique to quickly fabricate novel heat sink designs. The performance characteristics of two conventional and three novel heat sink designs fabricated using this technique will be presented.

1.1. Selective Laser Melting

Selective Laser Melting (SLM) is a layer-additive process that can fabricate metallic objects with a design defined by 3D model data. The process has featured in the work of Agarwala et al. [23], Childs et al. [24], Klocke et al. [25] and Kruth et al. [26] where material properties such as tensile strength, hardness and elongation were determined for bronze, commercially pure titanium and various steel alloys.

The apparatus used is the MCP Realizer II, a commercial SLM workstation with a 200 W continuous wave ytterbium fibre laser. The process takes place in a sealed argon atmosphere, to reduce oxidation and prevent fire, and involves the repetition of two steps to create a solid geometry layer by layer. Fig. 1 shows the main elements of the process. The component is manufactured, or 'built',

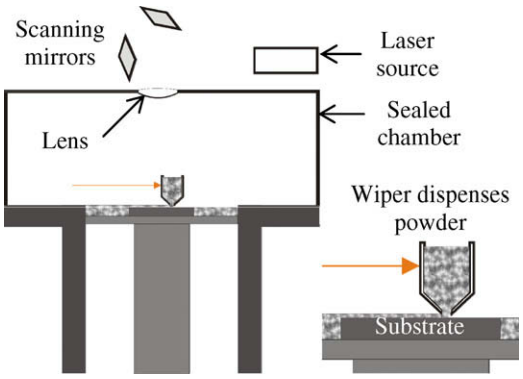

Fig. 1. Powder deposition.

onto a substrate that is often removed from the manufactured part at the end of the fabrication process. The substrate is attached to a piston whose position can be accurately controlled. In the first stage of the process a 50 μm thick layer of metallic powder with a particle size range of 10–53 μm is spread on the substrate by a moving hopper containing the feedstock metal powder. A laser is then fired at this powder layer (Fig. 2) traversing a pattern according to the slice of the 3D model data. The laser beam is positioned using dual axis mirrors and focussed through an f-theta lens. The moving laser beam fully melts the powder which quickly re-solid-

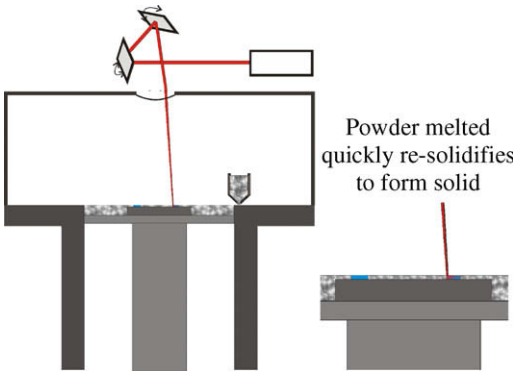

Fig. 2. Laser melting process.

ifies to form a slice of the entire model. The substrate is then lowered, another layer of powder deposited, and the process repeated.

The SLM process can fabricate components with features that cannot be produced by conventional manufacturing techniques. Examples of this include internal geometries (one shell inside another), reverse draft angles and fine detail. Wall thicknesses of 100 μm can be fabricated allowing small hydraulic diameters to be produced, which are known to offer a higher heat transfer per unit volume compared to larger channels [27] as shown in Jiang et al's [28] study on micro heat exchangers. There is also scope to alter the surface roughness of SLM-fabricated heat sinks. An increase in surface roughness is known to improve the heat transfer from a cylinder in cross flow [29].

Although the rapid prototyping industry has recognised that the SLM process is particularly suited to the production of extended surfaces for heat transfer applications, attention in the literature has previously focussed on the effect of the laser processing parameters on mechanical properties. A perceived weakness that has prevented the SLM process from being used more widely to fabricate heat sinks is the poor thermal conductivities of the materials used, which are in the range of 18–22 W/m K. A recent advance was made by Wong et al. [30] where aluminium 6061, which has a bulk thermal conductivity of 170 W/m K, was successfully used with the SLM process. Although components produced in that study were only 90% dense and the effective thermal conductivity was just 70 W/m K, this is a significant improvement on the thermal conductivities of other materials commonly used with the SLM process.

The heat sinks in this paper take advantage of SLM's ability to produce complex three-dimensional geometries with fine details to demonstrate the suitability of the process for producing a new generation of heat sinks. The following sections will describe the heat sinks under investigation and compare their pressure drop and heat transfer performance to each other and to the characteristics of traditional offset strip fins that are available in the literature.

2. Experimental techniques

2.1. Heat sink geometries

Five heat sink geometries were manufactured from aluminium 6061 using the SLM process. Two of these were offset strip fins, one with rectangular fins, and the other rounded rectangular fins, labelled Rectangle and Rect RND, respectively. The other heat sinks consisted of an elliptical array, a pin fin array and a lattice, labelled Ellipse, Pin fin 6061 and Lattice respectively. The lattice structure is typical of a rapid prototyping support structure used to fix the part being manufactured to a substrate; it is often removed and discarded after the fabrication process is complete but in this investigation it serves as an example of how the SLM process can be used to fabricate high surface area to volume heat sinks. With reference to Fig. 3, it is clear that all but Pin fin 6061and Rectangle would be difficult if not impossible to manufacture using traditional manufacturing processes. The dimensions of these heat sinks are given in Fig. 4 and Table 1; the air flow and pin heights are in the z and y directions respectively. The overall dimensions of the heat sinks shown in Fig. 3 are 50 mm by 10 mm by 100 mm for the width, height and length respectively. It is the fine detail and small inter-pin distances that make it difficult to manufacture these designs using conventional processes.

The fin arrays in this investigation are designed for use within shallow cavities such as electronics enclosure cold walls, which are commonly around 10 mm in height. This short height prevents the lower conductivity of the SLM fabricated heat sinks from having a significant effect on fin efficiency. For example, assuming a constant heat transfer coefficient of 100 W/m^2 K on its surface, Pin fin 6061 would have fin efficiencies of 96% and 91% if they were made from a cast aluminium 6061 and an SLM fabricated aluminium, respectively. The difference in fin efficiency due to the heat sinks thermal conductivity would be increased if the fin length was doubled, giving fin efficiencies of 75% and 87%. The results presented within this paper are only valid for heat sinks with a thermal conductivity of 70 W/m K.

At this early stage of the research, control of the surface roughness of aluminium 6061 heat sinks produced by SLM is not possible. However, the surface roughnesses of the heat sinks in this paper were measured to have an average roughness (R_a) of between 15 and 25 μm. The heat sinks can be fabricated in batches of three giving an average production time of one and a half hours per heat sink.

2.2. Experimental apparatus and test procedure

The heat sinks were fabricated on substrates made of extruded aluminium 6061 that can be seen in Fig. 3 with width 50 mm and

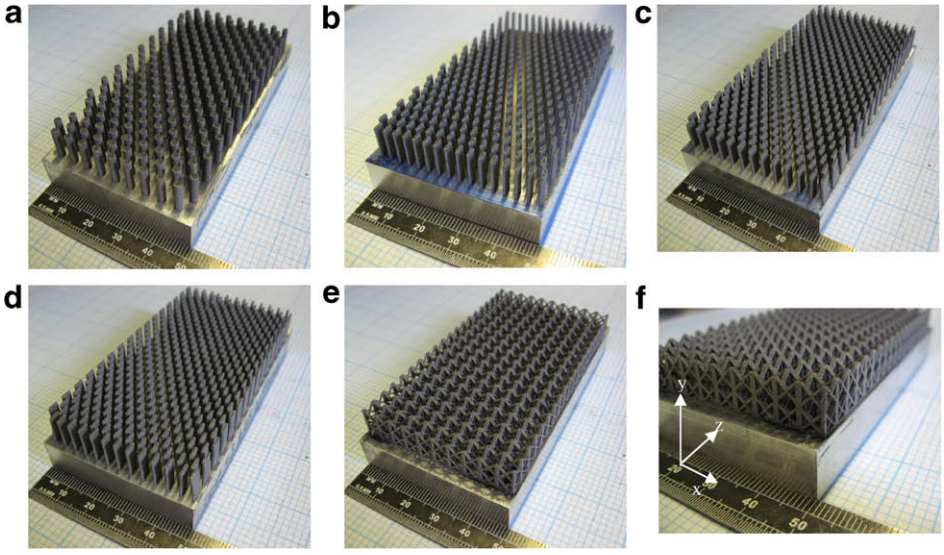

Fig. 3. SLM fabricated heat sinks, base dimensions 50 mm × 100 mm, flow in the z direction. (a) Pin fin 6061, (b) Rectangle, (c) Rect RND, (d) Ellipse, (e) Lattice and (f) close up of Lattice.

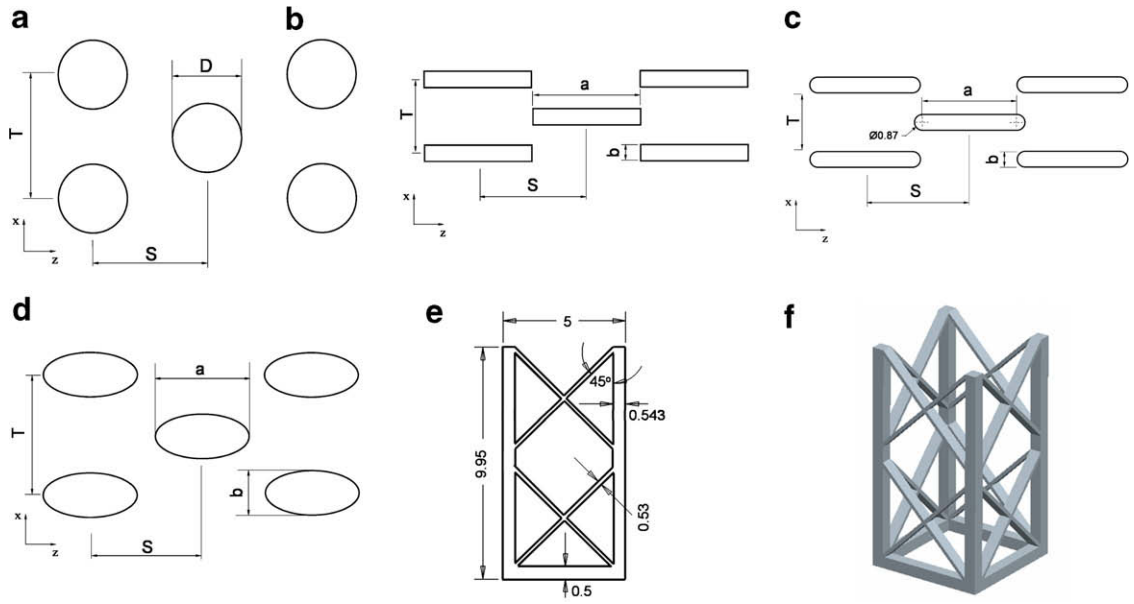

Fig. 4. Heat sink dimensions at pin base for (a) Pin fin 6061, (b) Rectangle, (c) Rect RND, (d) Ellipse, (e) Lattice and (f) Isometric view of one Lattice cell.

Table 1
Heat sink dimensions

Heat sink	Pin fin 6061	Rectangle	Rect RND	Ellipse	Lattice
S/(mm)	5.05	3.00	3.00	2.46	–
T/(mm)	3.87	3.82	3.82	3.90	–
a/(mm)	–	3.24	3.72	3.19	–
b or *D*/(mm)	2.21	0.87	0.87	0.96	–
Pin circumference/(mm)	6.94	8.23	9.19	6.99	–
Heat transfer surface area/(mm^2)	20,610	39,060	43,030	37,430	55,200
Surface area/volume/(mm^{-1})	0.41	0.78	0.86	0.75	1.10
Free flow area/(mm^2)	280	390	390	310	260
Number of pins	228	416	416	466	–

length 100 mm. By bolting these solid aluminium 6061 substrates to a 16 mm thick copper block heated by two 6 mm diameter electrical cartridge heaters a uniform temperature condition could be applied to the base. The temperature across the interface between the copper block and heat sink only varied by 0.5 °C.

Fig. 5 shows the experimental arrangement used to test the SLM heat sinks. The test piece and heater block were placed in the test section, which was insulated. The height and width of the test section was 10 and 50 mm, respectively and remained fixed. Air at ambient conditions was forced by a centrifugal blower through a flow straightener in a length of inlet duct equivalent to sixty hydraulic diameters to ensure that flow entering the test section was fully developed. Upon leaving the test section, the air travelled through another flow straightener and exit duct (with a length equivalent to twenty hydraulic diameters), entered a thermal mass flow meter and exited to atmosphere. The heat input and the flow rate of air delivered were controlled by varying the supply voltages to the cartridge heaters and blower. Temperatures and pressures were measured at the positions indicated in Fig. 5 (where T_{in}, T_{out} and T_b are the inlet, outlet and heat sink base temperatures, respectively). T_{out} was taken as the average value of an array of six thermocouples across the test section exit and T_∞ was defined as the average of T_{in} and T_{out}. The heat sink base temperature was taken to be the average of the six thermocouples located in the heat sink substrate. The properties of the cooling air were evaluated at the bulk mean temperature.

The heat transfer and pressure drop investigations were carried out separately to eliminate the effects of temperature-dependent fluid properties. In the heat transfer investigations the heat sink substrate was heated with a constant heat input

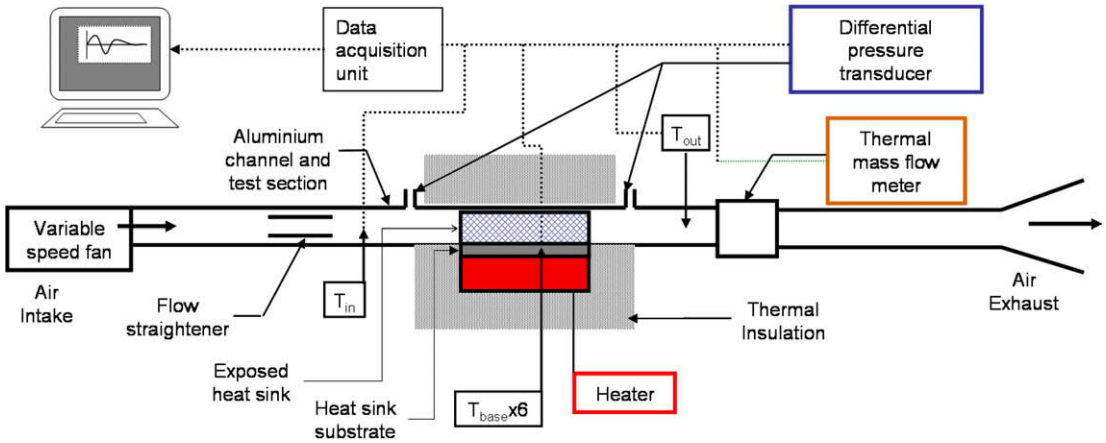

Fig. 5. Heat sink test apparatus.

and cooled with a fixed air flow rate. The flow rate and temperatures were then recorded at thirty second intervals. Upon T_{in}, T_{out} and T_b remaining constant (within 0.2 °C) for 10 min, the test was stopped.

The averages of the temperatures, pressures and flow rates taken over the steady-state 10 min interval were then taken as the result for that flow rate and heat flux. By maintaining substrate temperatures to within +30 °C of the ambient air temperature and applying insulation to the test section, the heat lost from the heat sinks due to radiation was minimised and ignored, as in similar investigations by Jubran et al. [31], Naik et al. [32] and Tahat et al. [10].

The pressure drop investigations were conducted with the heat sinks unheated. The flow rate was fixed and both the mass flow rate and pressure drop across the heat sink were recorded every 30 s for a period of 10 min. This provided robust mean values of temperatures, pressure drop and flow rate. The measurements were then averaged across the 10 min period. As the arrays consisted of 34 or more rows, the entry and exit losses that are associated with the flow through a pin array were considered negligible [33] compared to the pressure loss across the entire array.

An uncertainty analysis following the method of Kline and McClintock [34] showed that uncertainties in the Reynolds number and modified heat transfer coefficient were ±7% and ±18%, respectively at the 95% confidence level.

3. Results and discussion

3.1. Offset strip array

As this is the first time the heat transfer performance of heat sinks produced by SLM have been characterised, the offset strip array (Rectangle) was fabricated by SLM to provide a comparison with results that are available in the literature for similar geometries.

3.1.1. Heat transfer

There are several correlations available in the literature for heat transfer performance of offset strip arrays but those provided by Manglik and Bergles [35] were chosen as they are based on three separate studies by Kays and London [27], London and Shah [36], and Walters [37]. Results are presented in terms of the j factor:

$$j = \frac{Nu_{D_h}}{Re_{D_h} Pr^{1/3}} \tag{1}$$

where Nu is the Nusselt number:

$$Nu_{D_h} = \frac{hD_h}{k} \tag{2}$$

where h is the heat transfer coefficient:

$$h = \frac{\dot{m} c_p (T_{out} - T_{in})}{A(T_s - T_\infty)} \tag{3}$$

and D_h is the hydraulic diameter:

$$D_h = \frac{4A_{ff}L}{A} \tag{4}$$

The air flow rate is represented by the Reynolds number:

$$Re_{D_h} = \frac{\rho V_{ff} D_h}{\mu} \tag{5}$$

where V_{ff} is the mean velocity at A_{ff}.

Manglik and Bergles [35] presented heat transfer performance correlations in their study of offset strip arrays. Although the boundary conditions in the Manglik and Bergles investigation differ from the current study's, it was the closest representation of the current experiment that could be found in the literature. Whereas Manglik and Bergles use copper offset strips heated from both sides with a constant wall temperature, the current work uses a lower conductivity heat sink that is only heated from one side. Another difference between the test geometries in the Manglik and Bergles study and the current study is the geometry of the extended surface. Fig. 6 shows a traditionally manufactured offset strip array, where the top of the folded fin is attached to the heated surfaces and forms a feature that acts to enhance the heat transfer by increasing the frontal area visible to the approaching flow. This facet of the manufacturing process is not present on the SLM fabricated heat sinks.

Fig. 7 shows that the j factors for the SLM-fabricated heat sink are lower than the values described by the Manglik and Bergles correlation across the range of Reynolds numbers investigated. By comparing symmetrically and asymmetrically heated rectangular duct data from Kays and Crawford [38] the converging trends of the j factors with increasing Reynolds numbers can be explained. Kays and Crawford showed that for laminar flow the heat transfer was 53% higher for symmetrically heated walls compared to asymmetrically heated walls. Given the disparity in boundary conditions and materials used, the lower j factor of the currently study compared to Manglik and Bergles can be regarded as an acceptable difference.

3.1.2. Pressure drop

The pressure drop across the offset strip array in Fig. 7 is represented by f, the friction factor:

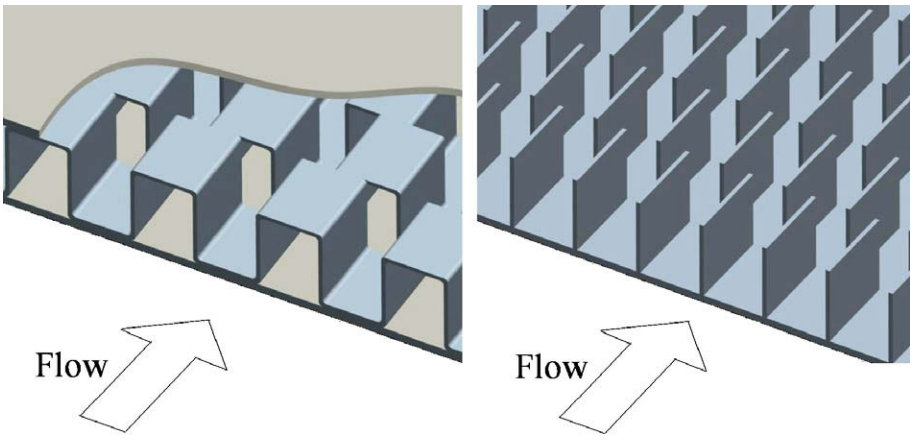

Fig. 6. Diagram of conventionally produced offset strip fins (left) and SLM-fabricated offset strip fins (right).

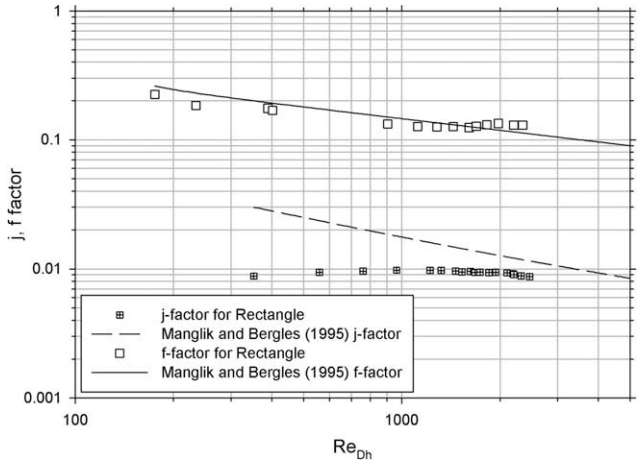

Fig. 7. Heat transfer and pressure drop performance of Rectangle compared to Manglik and Bergles [35].

$$f_{d,L} = \frac{\Delta p D_h}{1/2 \rho V_{ff}^2 L} \tag{6}$$

where Δp is the pressure drop across the array and L is the length of the heat sink.

Despite the geometric differences due to the differing manufacturing methods, the friction factors are within ±20% of the Manglik and Bergles correlation, which is also the accuracy they claimed for the correlations developed in their study. Effects such as the increased surface roughness of the SLM offset strip and the manufacturing variations in the folded offset strip fins, such as burred fin edges, both add to slight differences in results.

3.2. Comparison between SLM manufactured heat sinks

This investigation compares the performance of geometrically dissimilar shapes which makes it difficult to use dimensionless groups to compare the characteristics of the different geometries. The data will therefore be presented in dimensional form.

3.2.1. Heat transfer performance

To faithfully represent which of the extended surfaces considered is able to transfer the most heat, a modified heat transfer coefficient is used:

$$h_{mod} = \frac{\dot{m} c_p (T_{out} - T_{in})}{A_{prime}(T_s - T_\infty)} \tag{7}$$

where A_{prime} is the surface area of the heat sink base, which in this investigation is fixed at 5000 mm^2. This replaces the commonly used heat transfer surface area which skews the heat transfer performance measure in favour of heat sinks with smaller surface areas. In a design situation, the pressure drop performance and heat transfer characteristics are the relevant criteria by which an extended surface is selected, the heat transfer surface area need not be considered. The heat transfer performances of the five aluminium 6061 heat sinks in this investigation are presented in Fig. 8. The traditional heat transfer coefficient, based on the wetted heat transfer surface area, A, is presented in Fig. 9 to illustrate the difficulty interpreting heat transfer data based on this parameter. Fig. 8 clearly shows that Pin fin 6061 ranks fourth in terms of the amount of heat dissipated, yet Fig. 9 implies that it dissipates the most heat out of the heat sinks investigated.

Fig. 8 shows that Rect RND and Rectangle both dissipate more heat than the other heat sinks considered with Rect RND dissipating marginally more than Rectangle. The similarity in performance

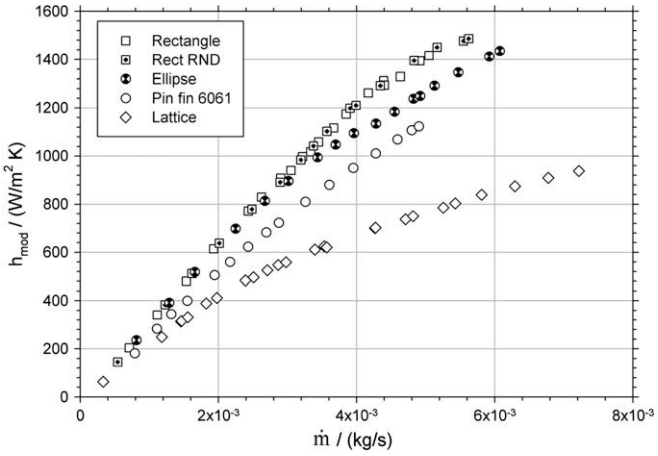

Fig. 8. Heat transfer coefficient based on prime surface area.

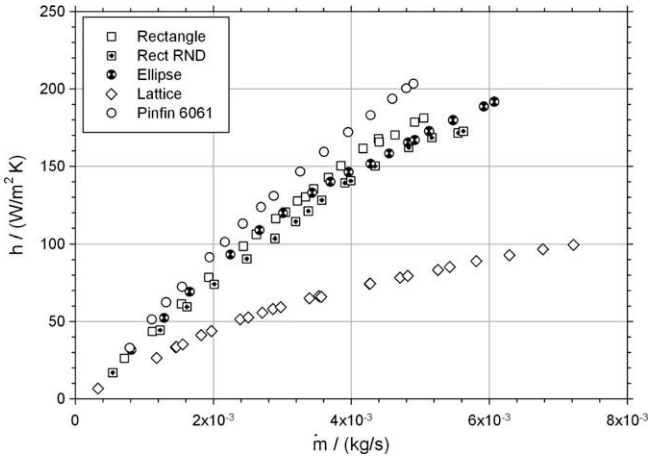

Fig. 9. Heat transfer coefficient based on heat transfer surface area.

of these two geometries is expected since the fluid flow through each is similar.

Lattice clearly demonstrates that increasing the heat transfer surface area does not necessarily bring about an improvement in heat transfer. At 4.3×10^3 kg/s it can dissipate only 54% of the heat that Rect RND can, yet it has a 28% larger heat transfer surface area. There are two causes of Lattice's poor performance. First, the low thermal conductivity material and thin sections ensure that each strut within the lattice has a large temperature gradient across it resulting in a poor fin efficiency. Second, although the lattice is complex there are channels aligned with the flow for the length of the heat sink, see Fig. 10, thus allowing air to travel through without much interaction with the structure. The wakes behind the upstream rows of Lattice act to shadow downstream struts from the flow, thereby reducing the heat transferred from each. When these two effects are combined, much of the heat transfer surface area becomes ineffective.

Although the heat transfer surface areas of Ellipse and Rectangle are similar, at higher flow rates the offset strips offer a 12% increase in heat transfer. The heat transfer performances begin to differ at 2.4×10^{-3} kg/s which corresponds to a Reynolds number (based on the hydraulic diameter of Rectangle) of 1200. The studies of Joshi and Webb [12] and De Jong et al. [11] place this flow rate just above the laminar/turbulent transition region for offset strip fins, suggesting that the vortices that begin to shed from rectangular fins at this flow rate are not shed from the streamlined elliptical

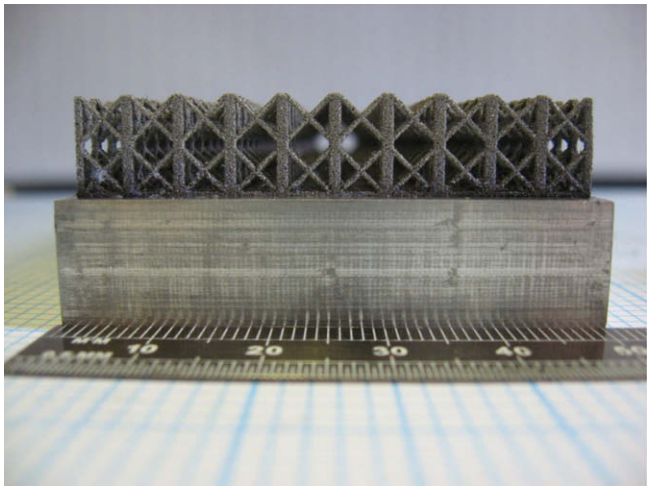

Fig. 10. Lattice viewed from the direction of the approaching cooling air.

fins. Flow visualisations from De Jong and Jacobi [39] for mass transfer analyses on offset strips confirmed that the onset of significant vortex shedding coincides with a marked increase in convective transport.

Pin fin 6061 is included in Fig. 8 to provide a comparison with a heat sink of conventional geometry. Although it does not perform as poorly as Lattice, its low heat transfer area limits its modified heat transfer coefficient. Improvements in heat transfer may be gained from increasing fin density, although excessive pressure losses across the pin fin array inhibits this course of action, as shown in the next section. Although the elliptical and cylindrical arrays were not optimised, the heat transfer results confirm the findings of Matos et al. [15]; Ellipse transfers an additional 13% heat when compared to Pin fin 6061.

3.2.2. Pressure drop performance

The pressure loss across Pin fin 6061, shown in Fig. 11, highlights the reason why increasing the pin number to improve heat transfer from a cylinder array is not a viable option in this case. The vortex shedding within cylinder arrays may act to improve heat transfer and mixing of the flow but coupled with wake losses, it also increases pressure losses.

The effect of wake losses on the pressure drop across an array can be seen by comparing Rectangle and Rect RND. Despite the slightly increased surface area, the superior aerodynamic profile of Rectangle RND gives it a lower form drag that aids pressure recovery in the wake of each fin. The difference in pressure drop between the two geometries increases at higher flow rates as the inertia forces begin to dominate.

The elliptical array incurs the lowest pressure drop out of the geometries investigated. Ellipse has a surface area comparable to Rectangle, but at a mass flow rate of 5.4×10^{-3} kg/s the offset strip has a 57% higher pressure drop across it. Given that the free flow area of Ellipse is also smaller than Rectangle, the reduction in pressure losses due to the use of an elliptical pin can only be attributable its superior aerodynamic profile. Matos et al. [15] found that the pressure drop across an optimised elliptical array was 25% less than that across an optimised cylindrical array. In this investigation, where the arrays are not optimised but do share similar pin circumferences and transverse pin spacings, the elliptical array pressure loss is only 40% of the cylindrical array pressure loss.

Based on the large surface area and low free flow area of the Lattice heat sink it may be expected that the pressure drop across it would be the largest of the heat sinks investigated, yet it is placed between Rectangle and Rect RND. Returning to Fig. 10, the low pressure loss can be seen to be due to the channels within the lattice which allow air to flow through, undeviated. Recirculation zones behind each strut may incur a slight pressure loss, but these wakes also guide incoming air to the straight-through, hence reducing the pressure loss as well as the extended surface's heat transfer performance.

3.3. Heat sink performance

The pressure drop and heat transfer characteristics are often equally important when designing a heat sink. For this reason the performance indicies based on the ratio of the modified heat transfer coefficient and the pressure loss are presented in Fig. 12.

Both Pin fin 6061 and Lattice perform poorly compared with the other extended surfaces, but for different reasons. Whereas the pin fin arrangement is capable of reasonable heat transfer, it also suffers from large pressure losses; the lattice has poor heat transfer performance but offers little resistance to the the air flow.

The improvement made to the traditional offset strip design by rounding the corners can be seen throughout the majority of the experimental flow range. By reducing pressure losses behind each strip the reduced pumping power required for Rect RND will reduce energy consumption and the noise produced by cooling fans. By reducing the volume of recirculation zones and removing sharp edges, the design may also offer a reduction in fouling rates.

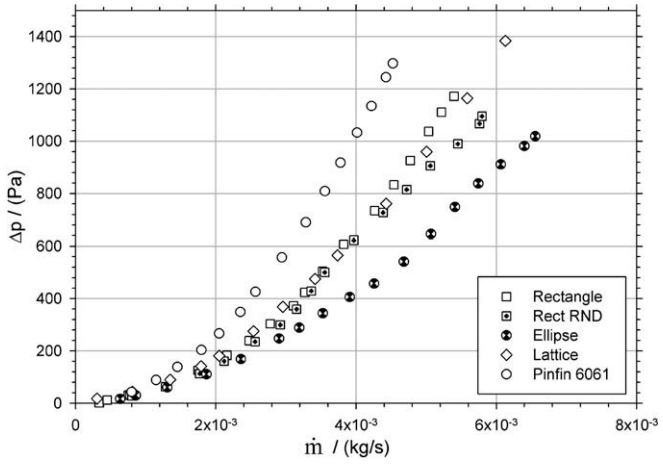

Fig. 11. Pressure drop across heat sinks.

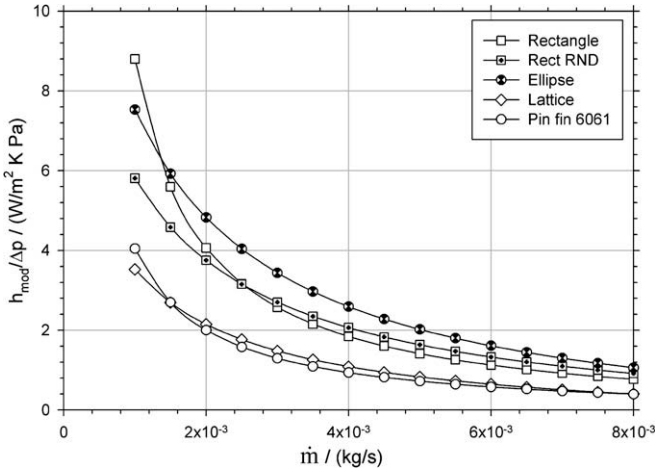

Fig. 12. SLM heat sink efficiency index.

The elliptical array offers the most effective performance out of the heat sinks investigated. Elliptical pins can be assembled in an array to create a large heat transfer surface area per unit volume whilst maintaining an acceptable pressure drop. Further investigation is required to determine whether the elliptical arrays offer even greater improvement over offset strips when parameters such as pin thickness, length and spacing are varied.

4. Conclusions

The rapid fabrication technique of Selective Laser Melting has been introduced and the heat transfer and pressure drop characteristics of five heat sinks have been presented. The heat sinks investigated were chosen to demonstrate SLM's ability to produce complex three-dimensional structures with features that would be difficult if not impossible to manufacture using conventional methods. A lattice-structure heat sink demonstrated that increasing the heat transfer surface area alone does not necessarily improve overall heat transfer performance; the coolant path through the lattice must also be carefully considered.

The air flow through an offset strip array was improved by adding rounded ends to the fins. This was simple to implement using the SLM process but offered a noticeable reduction in pressure loss across the offset strip fins, without incurring a reduction in heat transfer performance. An extension of the offset strip was an array of elliptical fins which offered the highest heat transfer rate per unit pressure drop compared to the other extended surfaces tested.

The heat sinks considered in this investigation have not been optimised, yet they clearly demonstrate the performance enhancements that SLM can bring to heat sink design. The manufacturing lead time of the SLM process means that prototypes can be designed, manufactured and tested in relatively short timescales.

Acknowledgement

The support of The Engineering and Physical Sciences Research Council through grant GR/S98405/01 and SELEX Sensors and Airborne Systems Ltd. is gratefully acknowledged.

References

[1] A. Zukausakas, Convective heat transfer in cross flow, in: S. Kacac, R.K. Shah, W. Aung (Eds.), Handbook of Single-Phase Convective Heat Transfer, Wiley-Interscience, New York, 1987. Chapter 6.
[2] B.A. Brigham, G.J. VanFossen, Length to diameter ratio and row number effects in short pin fin heat transfer, Journal of Engineering for Gas Turbines and Power 106 (1987) 241–245.
[3] D.E. Metzger, Z.X. Fan, W.B. Shephard, Pressure loss and heat transfer through multiple rows of short pin fins, Heat Transfer 3 (1982) 137–142.
[4] Y. Peng, Heat transfer and friction loss characteristics of pin fin cooling configurations, Transactions of the ASME: Journal of Engineering for Gas Turbines and Power 106 (1984) 246–251.
[5] J. Armstrong, D. Winstanley, A review of staggered array pin fin heat transfer for turbine cooling applications, Journal of Turbomachinery 110 (1988) 94–103.
[6] R.F. Babus'Haq, K. Akintunde, S.D. Probert, Thermal performance of a pin-fin assembly, International Journal of Heat and Fluid Flow 16 (1995) 50–55.
[7] B.E. Short, P.E. Raad, C.D. Price, Performance of pin fin cast aluminium coldwalls part 1: friction factor correlations, Journal of Thermophysics and Heat Transfer 16 (3) (2002) 389–396.
[8] E.M. Sparrow, J.W. Ramsey, C.A.C. Altemani, Experiments on in-line pin fin arrays and performance comparisons with staggered arrays, Transactions of the ASME: Journal of Heat Transfer 102 (1980) 44–50.
[9] M. Tahat, R.F. Babus'Haq, S.D. Probert, Forced steady-state convections from pin-fin arrays, Applied Energy 48 (1994) 335–351.
[10] M. Tahat, Z.H. Kodah, B.A. Jarrah, S.D. Probert, Heat transfers from pin-fin arrays experiencing forced convection, Applied Energy 67 (2000) 419–442.
[11] N.C. DeJong, L.W. Zhang, A.M. Jacobi, S. Balachandar, D.K. Tafti, A complementary experimental and numerical study of the flow and heat transfer in offset stri-fin heat exchangers, Transactions of the ASME: Journal of Heat Transfer 120 (1998) 690–698.
[12] H.M. Joshi, R.L. Webb, Heat transfer and friction in the offset strip fin heat exchanger, International Journal of Heat and Mass Transfer 30 (1987) 69–84.
[13] L.W. Zhang, S. Balachandar, D.K. Tafti, F.M. Najjar, Heat transfer enhancement mechanisms in inline and staggered parallel-plate fin heat exchangers, International Journal of Heat and Mass Transfer 40 (10) (1997) 2307–2325.
[14] M. Iyengar, A. Bar-Cohen, Design for manufacturability of SISE parallel plate forced convection heat sinks, IEEE Transactions on Components and Packaging Technologies 24 (2) (2001) 150–158.
[15] R.S. Matos, J.V.C. Vargas, T.A. Laursen, F.E.M. Saboya, Optimization study and heat transfer comparison of staggered circular and elliptic tubes in forced convection, International Journal of Heat and Mass Transfer 44 (2001) 3953–3961 .
[16] Z. Chen, Q. Li, H. Meier, J. Warnecke, Convective heat transfer and pressure loss in rectangular ducts with drop-shaped pin fins, Heat and Mass Transfer 33 (1997) 219–224.
[17] A.F. Bastawros, A.G. Evans, H.A. Stone, Evaluation of cellular metal heat dissipation media, Technical Report MECH 325, DEAS Harvard University, 1998.
[18] T.J. Lu, Ultralight porous metals: from fundamentals to applications, Acta Mechanica Sinica 18 (5) (2002) 457–479.
[19] C.Y. Zhao, T. Kim, T.J. Lu, H.P. Hodson, Thermal transport in high porosity cellular metal foams, Journal of Thermophysics and Heat Transfer 18 (3) (2004) 309–317.
[20] T. Kim, C.Y. Zhao, T.J. Lu, H.P. Hodson, Convective heat dissipation with lattice-frame materials, Mechanics of Materials 36 (2004) 767–780.
[21] T. Kim, H.P. Hodson, T.J. Lu, Fluid-flow and endwall heat-transfer characteristics of an ultralight lattice-frame material, International Journal of Heat and Mass Transfer 47 (2004) 1129–1140.
[22] T. Kim, H.P. Hodson, T.J. Lu, Contributions of vortex structures and flow separation to local and overall pressure and heat transfer characteristics in an ultralightweight lattice material, International Journal of Heat and Mass Transfer 48 (2005) 4243–4264.
[23] M. Agarwala, D. Bourell, F. Beaman, H. Marcus, F. Barlow, Direct selective laser sintering of metals, Rapid Prototyping Journal 1 (1995) 26–36.
[24] T.H.C. Childs, C. Hauser, M. Badrossamay, Selective laser sintering (melting) of stainless and tool steel powders: experiments and modelling, Proceedings of IMechE – Part B, Journal of Engineering Manufacture 219 (2005) 339–357.
[25] F. Klocke, H. Wirtz, W. Meiners, Direct manufacturing of metal prototypes and prototype tools, in: Proceedings of 7th Solid Freeform Fabrication Symposium, Austin, Texas, 1996, pp. 141–148.
[26] J.P. Kruth, L. Froyen, J. Van Vaerenbergh, P. Mercelis, M. Rombouts, B. Lauwers, Selective Laser Melting of iron-based powder, Journal of Material Processing Technology 149 (2004) 616–622.
[27] W.M. Kays, A.L. London, Compact Heat Exchangers, 2nd ed., McGraw-Hill, New York, 1964.
[28] Pei-Xue Jiang, Ming-Hong Fan, Si Guang-Shu, Ren Ze-Pei, Thermal-Hydraulic performance of small micro channel and porous media heat exchangers, International Journal of Heat and Mass Transfer 44 (2001) 1039–1051.
[29] E. Achenbach, The effect of surface roughness on the heat transfer from a circular cylinder to the cross flow of air, International Journal of Heat and Mass Transfer 20 (1977) 359–369.
[30] M. Wong, S. Tsopanos, I. Owen, C.J. Sutcliffe, Selective laser melting of heat transfer devices, Rapid Prototyping Journal 13 (5) (2007) 291–297.
[31] B.A. Jubran, M.A. Hamdan, R.M. Abdualh, Enhanced heat transfer, missing pin, and optimization for cylindrical pin arrays, Transactions of the ASME: Journal of Heat Transfer 115 (1993) 576–583.
[32] S. Naik, S.D. Probert, M.J. Shilston, Forced convective steady state heat transfer from shrouded vertical fin arrays, aligned parallel to an undisturbed air stream, Applied Energy 26 (1987) 137–158.
[33] E.M. Sparrow, V.B. Grannis, Pressure drop characteristics of heat exchangers consisting of diamond-shaped pin fins, International Journal of Heat and Mass Transfer 34 (3) (1990) 589–600.
[34] S.J. Kline, F.A. McClintock, Describing uncertainties in single-sample experiments, Mechanical Engineering 75 (1953) 3–8.
[35] R.M. Manglik, A.E. Bergles, Heat transfer and pressure drop correlations for the rectangular offset strip fin compact heat exchanger, Experimental Thermal and Fluid Science 10 (1995) 171–180.
[36] A.L. London, R.K. Shah, Offset rectangular plate-fin surfaces- heat transfer and flow friction characteristics, Transactions of the ASME: Journal of Engineering Power 90 (1968) 218–228.
[37] F.M. Walters, Hypersonic research engine project- phase IIA, Category I Test Report on fin heat transfer and pressure drop testing, Data Item No. 63.02, AiResearch Manufacturing Co. Doc. AP-69-5348, 1969.
[38] W.M. Kays, M.E. Crawford, Convective Heat and Mass Transfer, McGraw-Hill, New York, 1980.
[39] N.C. DeJong, A.M. Jacobi, An experimental study of flow and heat transfer in parrallel-plate arrays: local, row-by-row and surface average behaviour, International Journal of Heat and Mass Transfer 40 (6) (1997) 1365–1378.